



Delft University of Technology

Concentration polarizations of PEG and silica colloids in ceramic nanofiltration

Zhang, Shuo; Liang, Yixin; Yang, Cai; Venema, Paul; Rietveld, Luuk C.; Heijman, Sebastiaan G.J.

DOI

[10.1016/j.desal.2024.117722](https://doi.org/10.1016/j.desal.2024.117722)

Publication date

2024

Document Version

Final published version

Published in

Desalination

Citation (APA)

Zhang, S., Liang, Y., Yang, C., Venema, P., Rietveld, L. C., & Heijman, S. G. J. (2024). Concentration polarizations of PEG and silica colloids in ceramic nanofiltration. *Desalination*, 583, Article 117722.
<https://doi.org/10.1016/j.desal.2024.117722>

Important note

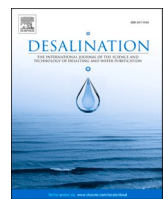
To cite this publication, please use the final published version (if applicable).
Please check the document version above.

Copyright

Other than for strictly personal use, it is not permitted to download, forward or distribute the text or part of it, without the consent of the author(s) and/or copyright holder(s), unless the work is under an open content license such as Creative Commons.

Takedown policy

Please contact us and provide details if you believe this document breaches copyrights.
We will remove access to the work immediately and investigate your claim.



Concentration polarizations of PEG and silica colloids in ceramic nanofiltration

Shuo Zhang^{a,*}, Yixin Liang^a, Cai Yang^b, Paul Venema^b, Luuk C. Rietveld^a, Sebastiaan G. J. Heijman^a

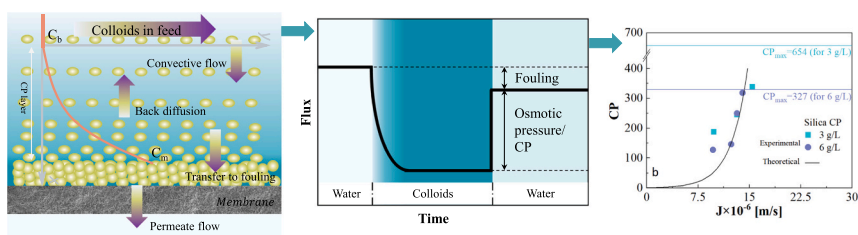
^a Section of Sanitary Engineering, Department of Water Management, Faculty of Civil Engineering and Geosciences, Delft University of Technology, Stevinweg 1, 2628 CN Delft, the Netherlands

^b Laboratory of Physics and Physical Chemistry of Foods, Wageningen University, Bornse Weilanden 9, 6708 WG Wageningen, the Netherlands

HIGHLIGHTS

- Flux decline caused by fouling and CP of colloids in ceramic NF was distinguished.
- CP was measured by the osmotic pressures in the feed and near the membrane wall.
- CP of silica colloids can reach up to 460.
- The high CP was the result of the slow back diffusion of colloids.
- CP of colloidal particles led to a maximum flux loss of 95 %.

GRAPHICAL ABSTRACT



ARTICLE INFO

Keywords:
Concentration polarization
Fouling
Colloid
Flux decline
Nanofiltration

ABSTRACT

A large decrease in permeability is often observed during the filtration of nano-sized colloids, while fouling is widely regarded as the main explanation for this phenomenon. The osmotic pressure or concentration polarization (CP) of colloids can also contribute to the flux decline. However, the contribution of CP to flux loss cannot be determined by the traditional CP model. In this study, the effect of fouling and CP/osmotic pressure on flux was distinguished. The CP values of polyethylene glycol (PEG) and silica-colloids were determined by the osmotic pressures near the membrane surface and in the feed. The CP induced by colloids accounted for 43–95% of the flux loss in our experiments. Silica exhibited higher CP values (127–460), compared to 7–71 for PEG. This was attributed to the slower back diffusion caused by the larger colloids, as evidenced by the diffusion coefficients of $4.30 \times 10^{-11} \text{ m}^2/\text{s}$ for silica (10 nm) and $1.45 \times 10^{-10} \text{ m}^2/\text{s}$ for PEG (2.9 nm). Although the CP was mitigated by increasing the cross-flow velocity, CP values of 31 and 250 were observed for PEG and silica at high Reynolds number of 7317, respectively. The experimentally obtained CP values were also compared with those calculated by the film diffusion model.

1. Introduction

During the filtration by pressure-driven membranes, such as reverse

osmosis (RO) and nanofiltration (NF), a transmembrane pressure as the driving force is applied onto the membrane, and particles and dissolved components will be retained on the feed side [1]. However,

* Corresponding author at: Department of Water Management, Faculty of Civil Engineering and Geosciences, Delft University of Technology, Stevinweg 1, 2628 CN Delft, the Netherlands.

E-mail address: S.Zhang-10@tudelft.nl (S. Zhang).

concentration polarization (CP) inevitably occurs during this filtration process, leading to the accumulation of dissolved compounds and colloidal particles near the membrane surface. This will potentially result in a decrease in permeability of the membrane [2,3]. Therefore, understanding CP is important for the interpretation of permeability decrease when filtering dissolved compounds and colloids [4–6].

Colloidal particles are prevailing in the aquatic environment and can have either an organic or an inorganic composition in a size range from 1 to 1000 nm [7]. During filtration of feedwater containing colloids, the membrane is prone to a considerable flux decline. Although colloidal fouling would not result in a high resistance increase due to the relatively large size of colloids compared to the pore size of the NF membrane, the CP of colloids near the membrane surface can cause a sharp rise in the osmotic pressure potentially affecting the permeability of the membrane [8–11]. Elimelech and Bhattacharjee have demonstrated that the CP for 2 nm-size rigid hard spherical particles in crossflow filtration was around 300 at a feed pressure of 4 bar [12]. It has also been revealed that the CP of bovine serum albumin and lysozyme in RO membrane could reach up to a value of 4645 and 612, respectively [9]. In addition, CP values of around 300 have been found for macromolecular polymers in polymeric NF [10], RO [13], and ultrafiltration membranes [14]. Although high CP values were revealed in filtration of macromolecule, flux decline was attributed more to fouling because the contribution of CP to flux decline cannot be quantified from the traditional model like the film diffusion model used for CP calculation. Moreover, for practical applications, mitigation of fouling and CP/osmotic pressure phenomenon can be completely different. Fouling is normally removed by the cleaning such as forward flush, backwash, and chemical cleaning, while CP mitigation can be achieved by: a) increase turbulence in order to decrease the CP-layer near the membrane surface, b) decrease permeate flux, and c) decrease concentration of colloids in the feed. Hence, it is also important to understand the effect of fouling and CP/osmotic pressure on permeability decrease for practice.

The film diffusion model is widely used in the rejection of molecules (ions etc.) to estimate the CP [2,10,15,16]. In a membrane system, the convective flow drives solutes towards the membrane and at the same time the solutes are rejected by the membrane. These solutes (ions, molecules, or colloids) also move away from the membrane surface owing to back diffusion. The phenomenon is depicted in Fig. 1a. Hence, when reaching equilibrium, this solute transport can be described by the following solute mass balance equation (Eq. (1)) [10]:

$$JC = D \frac{dC}{dx} + JC_p \quad (1)$$

where J is the flux (m/s), D is the solute diffusion coefficient in the solvent (m^2/s), x is the distance from the membrane surface (m), C and C_p are concentrations of solute near the membrane surface and permeate side (g/L), respectively. Integrating Eq. (1) towards a boundary layer

condition gives Eq. (2) [2]:

$$\beta = \frac{C_m - C_p}{C_b - C_p} = \exp\left(\frac{J \delta}{D}\right) = \exp\left(\frac{J}{K}\right) \quad (2)$$

where δ is the thickness of the boundary layer near the membrane (m), K is the mass transfer coefficient (m/s) in the boundary layer, β is the CP factor, C_m and C_b are the solute concentrations near the membrane surface and in bulk (g/L), respectively. If the size of the solute is larger than the membrane pore size, the solute is completely rejected by the membrane, and as a result, C_p is equal to zero. In this case, the CP factor can be described by Eq. (3) [16]:

$$\beta = \frac{C_m}{C_b} = \exp\left(\frac{J}{K}\right) \quad (3)$$

The mass transfer coefficient K in Eq. (3) is generally determined by the Sherwood equation (Eq. (4)) [15]:

$$Sh = \frac{K d_h}{D} = a Re^b Sc^c = a \left(\frac{u d_h}{v}\right)^b \left(\frac{v}{D}\right)^c \quad (4)$$

where Sh is the Sherwood number, Re is the Reynolds number, Sc is the Schmidt number, a, b, c are empirical constants, u is the flow velocity (m/s), d_h is the (tubular) hydraulic diameter of the membrane channel (m), v is the kinematic viscosity of the fluid (m^2/s). However, when fouling deposits on the membrane surface (Fig. 1b), the solute mass balance described by Eq. (1) in the film diffusion model is not valid, because it does not involve the mass of fouling. Therefore, Eq. (1) should be re-formulated into Eq. (5) to include the fouling part [17]. A represents the ratio of the total mass turning into fouling, but it could be affected by the complex hydraulic conditions and the thermodynamics of the solute. Given that this phenomenon is dynamic and complicated, A is difficult to be measured or presumed [17]. In addition, the film diffusion model should also consider the effect of fouling on the CP and boundary layer thickness (δ) (Fig. 1a and b). The real δ^* (Fig. 1b) is probably only equal to δ for a clean membrane. Also, for the solute concentrations near the membrane surface (C_m and C_m^*), they should only be the same when no fouling was formed on surface.

$$JC = D \frac{dC}{dx} + JC_p + AJC \quad (5)$$

Most studies limit their focus on the influence of the caked-enhanced CP (CECP) which is caused by the enhanced osmotic pressure of the retained ions in the fouling layer [6,18]. So far, the effect of fouling itself on the CP has been neglected. However, a significant deviation in CP resulting from the film diffusion model has been found when employing a more accurate model like the finite element numerical model [2]. This deviation is particularly pronounced at low feed flow velocity and high flux [2,8,19–21]. In addition, a deviation between directly monitored

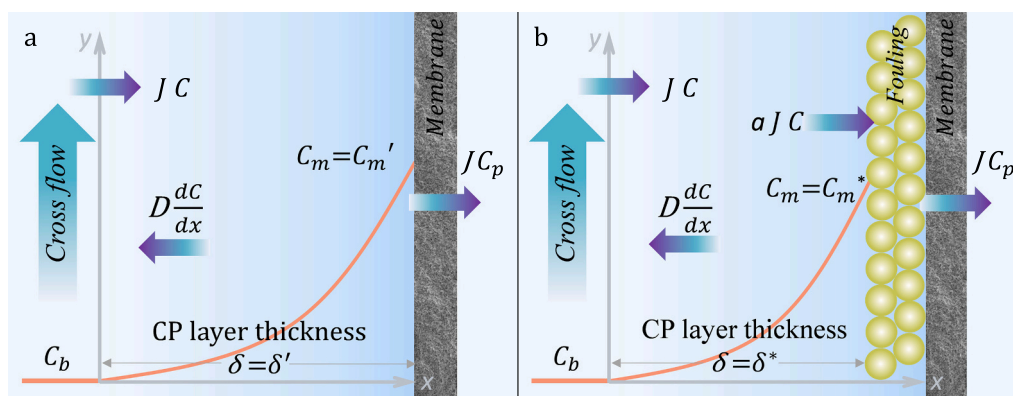


Fig. 1. CP profiles without (a) and with (b) fouling formation.

values and modelling results has been observed with respect to the CP profiles and the thickness of the boundary layer [8,22].

Fouling will not contribute to the osmotic pressure, hence the CP value can be predicted from the osmotic pressures near the membrane surface and in the feed. According to Van't Hoff's theory, osmotic pressure has a linear relation with the concentration for an ideal solution [23,24]. When all solutes are retained by the membrane, the permeate-side osmotic pressure is equal to zero. Therefore, CP can be expressed in Eq. (6):

$$\beta = \frac{C_m}{C_b} = \frac{\pi_m}{\pi_b} = \frac{\Delta\pi}{\pi_b} \quad (6)$$

where $\Delta\pi$ (Pa) is the osmotic pressure difference across the membrane, π_m and π_b are the osmosis pressures (Pa) on the membrane surface and in the bulk solution, respectively.

For a nonideal solution, the relation between osmotic pressure and concentration is nonlinear. However this nonlinear relationship is easily overlooked when the osmotic pressure is used in the prediction of CP by the traditional model [25–28]. To address this challenge, the above equation (Eq. (6)) is rewritten as shown in Eq. (7).

$$\beta = \frac{C_m}{C_b} = \frac{f(\Delta\pi)}{f(\pi_b)} \quad (7)$$

where $f(\Delta\pi)$ and $f(\pi_b)$ means that C_m and C_b are the functions of $\Delta\pi$ and π_b , respectively.

In order to contribute to the understanding of the role of CP enhanced osmotic pressure of colloids on the permeability of membranes, we developed a strategy to evaluate the CP generated by colloids and the flux loss only caused by CP in ceramic NF, while the effect of fouling on CP prediction was eliminated. To distinguish between the flux declines caused by fouling and CP, pure water flux was measured before and after filtration of colloids. The osmotic pressure generated near the membrane was also obtained via the above-mentioned method. Afterwards, the CP of two model colloids, polyethylene glycol (PEG) with a molecular weight of 6000 Da, and silica with a diameter of 10 nm, were obtained. A short-cycle filtration of colloids was also conducted to understand the effect of CP and fouling on flux decline, compared with a

long-cycle test. Given that the Sherwood equation is widely used in the film diffusion model for CP prediction, the theoretical results were compared with our experimental CP values. CP of colloids under various crossflows was also examined in this work.

2. Materials and methods

2.1. Filtration set-up and materials

Ceramic NF experiments were carried out in a crossflow setup, as shown in Fig. 2. Tanks 1 and 2 contained feed solutions of demineralized water and targeted solution, respectively, where a three-way valve was used to change the feed solutions. Two solutes of PEG (Sigma-Aldrich, Germany) with a molecular weight of 6000 Da, corresponding to 2.9 nm (Eq. (S1)), and silica (LUDOX® SM colloidal silica, Sigma-Aldrich, Germany) with an average particle diameter of 10 nm [29,30] were used. The commercial TiO₂ NF membrane (Inopor GmbH, Germany) had one channel of 7 mm internal diameter, 100 mm in length, and a porosity in the range of 30–40 %. The effective filtration area of the membrane was 0.000163 m². The ceramic NF had a measured molecular weight cut-off (MWCO) of 1623 Da (Fig. S1), corresponding to a pore size of 1.66 nm (Text S1), suggesting that both PEG and silica will be completely rejected.

2.2. Permeability declines caused by CP and fouling

CP is regarded as reversible phenomenon by removing colloids from the feed, while fouling, in the absence of cleaning (either hydraulic or chemical), is not, which can be observed through the flux decline [31,32]. Therefore, our experiments were divided into three parts (Fig. 3) to distinguish between the effect of fouling and CP on the permeability decrease of the membrane.

In the first step, demineralized water was filtrated over the pristine membrane. In this way, flux of the clean membrane can be expressed by Eq. (10):

$$J_w = \frac{\Delta P}{\mu_w R_m} \quad (10)$$

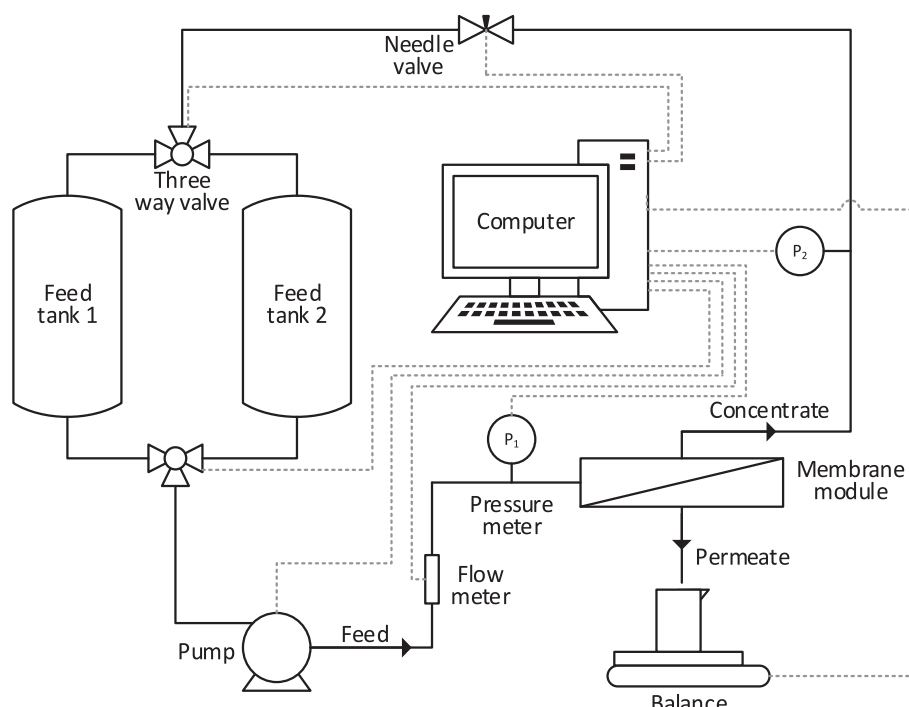


Fig. 2. Cross-flow filtration setup.

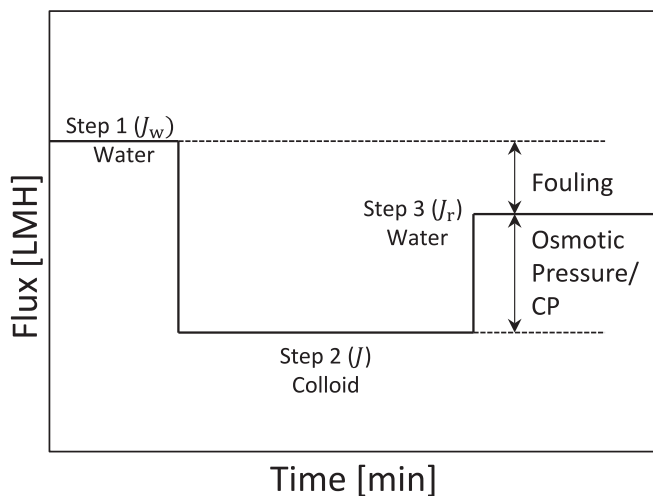


Fig. 3. Schematic diagram to separate the effect of fouling and osmotic pressure $\Delta\pi$ on flux, where step 1, 2, and 3 means the consecutive filtration of demineralized water with virgin membrane, targeted colloidal solution, and demineralized water in sequence.

where J_w is the permeate flux of demineralized water (m/s), μ_w is the dynamic viscosity of demineralized water (Pa s), R_m is the membrane resistance (1/m), and ΔP is the applied pressure (Pa). The permeability of the clean membrane during pure water filtration (L_w in m) is defined as the inverse of hydraulic membrane resistance, as shown in Eq. (11) [33]:

$$L_w = \frac{1}{R_m} = \frac{J_w \mu_w}{\Delta P} \quad (11)$$

In the second step, the solution, containing colloids, was filtrated at the same applied pressure, and therefore an extra osmotic pressure difference ($\Delta\pi$) occurred. Permeability (L in m) is the result of membrane resistance and fouling resistance (R_f in 1/m). In addition, the L can be described by flux (J in m/s), the dynamic viscosity of permeate-side solution (μ), and the effective transmembrane pressure ($\Delta P - \Delta\pi$). Hence, L is described by Eq. (12):

$$L = \frac{1}{R_m + R_f} = \frac{J \mu}{\Delta P - \Delta\pi} \quad (12)$$

In the final step, demineralized water was used again to measure the permeability of the fouled membrane (L_r in m) through the measured flux (J_r in m/s), as presented in Eq. (13). During this step, the concentration gradient on the membrane surface will be eliminated which means that the osmotic pressure disappeared, but membrane fouling still existed.

$$L_r = \frac{1}{R_m + R_f} = \frac{J_r \mu_w}{\Delta P} \quad (13)$$

During steps 2 and 3, the total resistances were caused by the membrane itself and fouling resistance, which means that L was equal to L_r [33]. Therefore, when Eq. (12) and 13 are combined, $\Delta\pi$ will be determined. Since the rejection by the NF membrane was complete, the values of $\Delta\pi$ and π_m were equal, and also the viscosities were equal: $\mu = \mu_w$ [34]. Hence $\Delta\pi$ can be obtained through Eq. (14):

$$\Delta\pi = \pi_m = \Delta P \left(1 - \frac{J}{J_r} \right) \quad (14)$$

2.3. Osmotic pressure

The relations between osmotic pressure and concentration of PEG and silica were shown in Fig. S2. The osmotic pressure equation

(Fig. S2a) for the PEG ($M_w = 6000$) was obtained from literature [35,36]. However, there is no proper relation between concentration and osmotic pressure of charged hard colloids like silica. This is because the counter ions in the diffuse double layer of the charged colloids also contribute to the osmotic pressure. The calculated osmotic pressure for uncharged hard spheres via Eq. (S3), described in Text S2, therefore always underestimates the osmotic pressure of charged hard spheres (Fig. S2b). Hence osmotic pressure of silica in this study was based on the virial expansion equation (Eq. (S2)) fitted with osmotic pressures measured by Osmomat 090 osmometer (Gonotec, Berlin, German), as described in Text S2 and shown in Fig. S2b.

3. Results and discussions

3.1. Effect of CP and fouling on flux decline

To distinguish between CP and fouling caused by colloidal particles, experiments were conducted with PEG and silica colloids, as described in the section of Materials and Methods. Detailed results of the conducted filtration experiments are given in Table 1. Prediction of CP via the film diffusion model (Eq. (3)) is normally based on the constant mass transfer coefficient of K calculated from Sherwood equation (Eq. (4)) [37]. However, various K values were found in our runs. Sutzkover et al. developed a method to evaluate K via the permeate flux before and after adding the trace salt [38]. However, their results gave a scattered image of the K values (e.g., 102 % error), even when the Re numbers and equipment geometries were similar. It was argued that K can be affected by the factors such as hydraulic conditions, viscosity, the concentration gradient, the suction effect, and solute-membrane interaction [20,34,38–42]. Hence, employing a constant K in the film diffusion model may limit the acquirement of an accurate CP. In addition, our results indicate that the osmotic pressure difference ($\Delta\pi$) between membrane surface and permeate side cannot be ignored, e.g., in the case of 10 g/L PEG, the induced $\Delta\pi$ was 2.80 bar accounting for 56 % of the applied pressure of 5.02 bar.

In addition, Fig. 4 shows the flux declined with time for (a) PEG, and (b) silica with different concentrations. The filtration was performed with pure water, colloidal solution, and pure water in sequence. Fig. 4a and b indicate that the initial flux declined with an increase in PEG or silica concentration, afterwards the flux tended to reach a plateau in all runs. The flux recovered rapidly when the feed was switched from a colloidal solution to pure water at the last step. The rapid, initial flux declines were probably attributed to the immediately generated osmotic pressure and adsorption of pollutants [43–49]. Wang and Song found that an equilibrium exists in membrane separation to reach a steady-state flux, and such flux will attain a lower plateau for the concentrated solution, which is in agreement with our finding [50]. The flux loss during moderate fouling would mainly be related to the gradual build-up and compression of the cake layer. At the last step where water was filtered over fouled membrane, colloids that raised the transmembrane osmotic pressure were flushed away with clean water, and therefore, the permeability was restored rapidly. However, the retained foulants on the membrane inhibited the flux to regain its initial performance.

Based on the effect of fouling and osmotic pressure on flux, the recovered part of the flux can be considered as the attribution of osmotic pressure, and the irreversible flux decline is the result of fouling, as explained in Fig. 3. In all series of operations, it is observed that the CP had a prominent impact on the flux loss, as shown in Fig. 4. The contribution of CP to the flux decline can be described by $(J_r - J)/(J_w - J) \times 100\%$. 95 % of flux loss due to CP was found in filtering 5 g/L PEG at 3 bar. Due to the high back diffusion of ions, CP of ions typically ranges from 1 to 2 in spiral-wound RO or NF treatment [51,52]. Consequently, these low CP values of ions have a limited effect on flux decline. However, as shown in Table 1, CP of 7–71 and 127–460 was found in filtration of PEG ad silica, respectively. The relatively high CP

Table 1

Experimental conditions and results of filtering PEG and silica in ceramic NF.

Feed	C_b , g/L	ΔP , bar	Flux, L/(m ² h)			π_b , bar	$\Delta\pi$, bar	C_m , g/L	K , $\times 10^{-6}$	CP
			Pure water (J_w)	Silica/PEG (J)	Pure water (J_r)					
PEG	1	1.58	36.5	33.7	35.2	4.2×10^{-3}	0.065	13.1	3.64	13.1
		3.05	68.1	61.2	65.7		0.211	32.8	4.87	32.8
		4.10	91.2	80.6	88.2		0.352	46.6	5.83	46.6
		5.40	125.3	97.9	112.1		0.684	70.5	6.39	70.5
	5	1.67	43.1	34.7	42.6	2.3×10^{-2}	0.311	42.9	4.48	8.6
		3.00	73.2	49.5	71.9		0.936	84.5	4.86	16.9
		4.00	94.1	53.5	82.5		1.404	105.5	4.88	21.1
		4.94	112.6	65.0	107.2		1.946	125.1	5.60	25.0
	10	1.65	42.2	24.6	39.1	5.0×10^{-2}	0.613	66.0	3.62	6.6
		3.00	72.8	36.7	69.2		1.410	105.7	4.32	10.6
		3.96	97.2	45.6	83.8		1.806	120.4	5.09	12.0
		5.02	120.6	45.8	103.7		2.804	150.2	4.69	15.0
Silica	3	1.52	45.0	35.3	40.2	4.5×10^{-5}	0.187	563.8	1.87	187.9
		2.27	65.2	47.4	55.1		0.316	736.8	2.39	245.6
		3.00	84.0	55.5	69.2		0.595	1015.7	2.65	338.6
		4.00	109.2	66.0	90.8		1.093	1380.0	2.99	460.0
	6	1.61	55.4	34.9	44.3	1.0×10^{-4}	0.340	764.2	2.00	127.4
		2.15	69.2	44.4	55.9		0.442	874.0	2.48	145.7
		3.17	99.9	47.6	80.0		1.286	1498.3	2.39	249.7
		4.10	125.1	50.4	102.5		2.083	1909.9	2.43	318.3

of colloids compared to ions thus exerted a more pronounced effect on flux decline. This finding suggests that in the NF of colloids, more attention should be paid to the CP and its potential effect on water production and fouling.

To further explore the impact of fouling and CP on flux decline, an additional short fouling cycle was employed before the long fouling cycle (Fig. 5a and b). During this experiment, demineralized water was filtered over a clean membrane for a few minutes, then the feed was adjusted to the colloidal solution for a short time (short fouling cycle), demineralized water, the colloidal solution for a longer time (long fouling cycle), and demineralized water, respectively. Here it is observed (Fig. 5) that the flux recovery of both PEG and silica during the first, short fouling cycle, was similar to that after the second, much longer, fouling cycle. This illustrates that colloidal fouling mainly formed at the beginning of the filtration. Moreover, a sharp flux loss also existed in this short-time fouling cycle, indicating that the effect of CP and fouling on flux behaviour occurred rapidly and simultaneously at the initial stage, with less dependence on filtration duration. The rapid formation of the CP layer in the initial phase of filtration has been directly monitored [53–55]. In addition, Hoek et al. [56] reported that in RO and NF, the increased osmotic pressure (i.e. enhanced by CP) was more significant compared to the negligible drop of hydraulic pressure across the fouling layer, thus dramatically reducing the driving force for flux.

3.2. Effect of applied pressure on CP

CP values of PEG (Mw = 6000) and silica were depicted in Figs. 6 and 7. Based on Eq. (14), the $\Delta\pi$ was obtained, afterwards the solute concentration near the membrane surface was determined by the relationship between osmotic pressure and concentration (Fig. S2a and b). Then, the CP values were calculated by the colloid concentrations near the membrane interface and in the feed.

It can be observed from Fig. 6a that CP increased with pressure for both PEG and silica. The driving force ($\Delta P - \Delta\pi$), increasing with the applied pressure, resulted in a higher flux. This will, in turn, lead to a higher CP, according to Eq. (2). Fig. 6a also shows that at a lower PEG concentration, pressure played a more important role in the CP increase, compared to the higher PEG concentration, e.g., the CP of 1 g/L PEG grew to 65.5 at 5.4 bar, 5.3 times higher than CP (i.e., 12.3) at 1.58 bar, while for 10 g/L PEG, the CP only increased 2.5 times when the applied pressures raised from 1.65 to 5.02 bar. In addition, Fig. 6a and b shows that the CP of silica (in the range of 127–460) was larger than when

filtering PEG (in the CP range of 7–71). Based on the Stokes-Einstein equation, larger particles have a smaller diffusion coefficient [57]. Compared with the high diffusion coefficient of ions (in the order of magnitude of 10^{-9} m²/s), the diffusion coefficients of PEG and silica were calculated at 1.45×10^{-10} and 4.30×10^{-11} m²/s, respectively. As a result, larger-size silica (10 nm, diameter) was prone to accumulation at the membrane surface on account of its low back diffusion, thus generating a higher CP than small-size PEG (2.9 nm, diameter). Similarly, such high CP indexes generated by macromolecules have been also discovered by groups of Elimelech [9,12], Ulbricht [10,13], and Tang [58].

3.3. Experimental and theoretical CP

Fig. 7 shows how flux correlated with the CP during membrane filtration. It indicates that for both PEG and silica, at a given flux, CP values were similar, e.g., the CP of 246 for 3 g/L silica at the flux of 1.13×10^{-5} m/s was comparable to 250 for 6 g/L silica at the flux of 1.13×10^{-5} m/s. This implies that CP was more affiliated with flux than bulk concentration, which has also been confirmed by literature [59]. Moreover, an increase in CP with flux was observed. For instance, CP increased 5 times, rising from 13 at 9.37×10^{-5} m/s to 71 at 2.72×10^{-5} m/s, in the case of 1 g/L PEG. This was because that the larger driving force due to the higher flux can lead to more accumulation of colloids near the membrane surface.

Evaluation of CP by the film diffusion model is also depicted in Fig. 7. The assessment was realized by employing various Sherwood equations from literature in the film diffusion model (dash lines in Fig. 7) [38,60–63]. The solid lines for both PEG and silica in Fig. 7 were based on our calibrated Sherwood equation ($Sh = 0.027 Re^{0.868} Sc^{0.25}$). The calibration was achieved by employing our experimental CP values in Eq. (3) to get the values of K (Table 1), then various values of K were used in Eq. (4) to calibrate the Sherwood equation. The calibrated Sherwood equation ($Sh = 0.027 Re^{0.868} Sc^{0.25}$) was comparable to the ones used in literature [38,60–63]. However, the deviation between experimental and theoretical CP values was observed. The CP deviation caused by the film model was also found when comparing to CP values which was obtained from the finite element numerical model [2]. As discussed in Introduction, the effect of fouling has not been considered in the film model, which can lead to the CP deviation. Besides, the constant K employed in the film diffusion model will also impact the acquirement of an accurate CP. As shown in Table 1, the K varied under different filtration conditions, which is consistent with the previous finding [38].

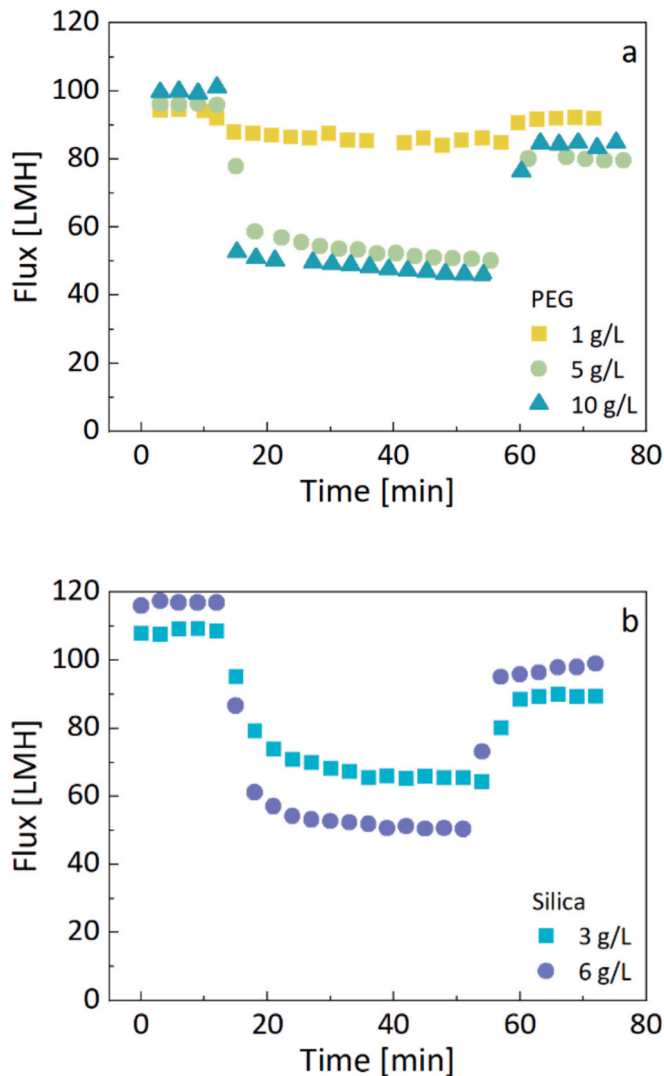


Fig. 4. Flux decline with the time of (a) PEG, and (b) silica-colloids with different concentrations for the distinction of the impact of fouling and osmotic pressure/CP on flux. The ceramic NF membrane was performed with water, colloidal solution, and water in sequence. All of the continuous operations were at a constant pressure of 4 bar, and a crossflow velocity of 0.5 m/s.

CP_{max} values in Fig. 7 referred to the theory of close-packing density [45]. Taking silica as an example, the maximal possible silica concentration should be 1961 g/L, when the close-packed volume fraction (74 %) was taken into account with an assumed silica density equal to 2650 g/L [45,64]. Therefore, the CP_{max} of 654 and 327 were obtained for 3 and 6 g/L silica, respectively. When the steady-state flux is reached, the CP layer will become constant. Once the colloidal concentration is higher than the CP_{max} [45,50,65], the extra colloids will be flushed away from the CP boundary layer or converted to fouling [47,51,53,66]. However, CP_{max} is not taken into consideration in the film diffusion model, thus leading to the high CP, e.g., 1694 for 3 g/L silica at the flux of 1.8×10^{-5} m/s, which was 3.7 times higher than the experimental CP (i.e., 460), and beyond CP_{max} (i.e., 654).

Our findings demonstrated that a high osmotic pressure near the membrane wall can be caused by colloids due to the high CP. The CP values given here were based on the fitted virial expansion equations used for the relation between osmotic pressure and concentration of the colloids (Text S2, Fig. S2a and b). However, for silica, when the osmotic pressure equation (Eq. (S3)) based on Carnahan-Stirling theory for hard-sphere particles was employed [67], completely different silica CP

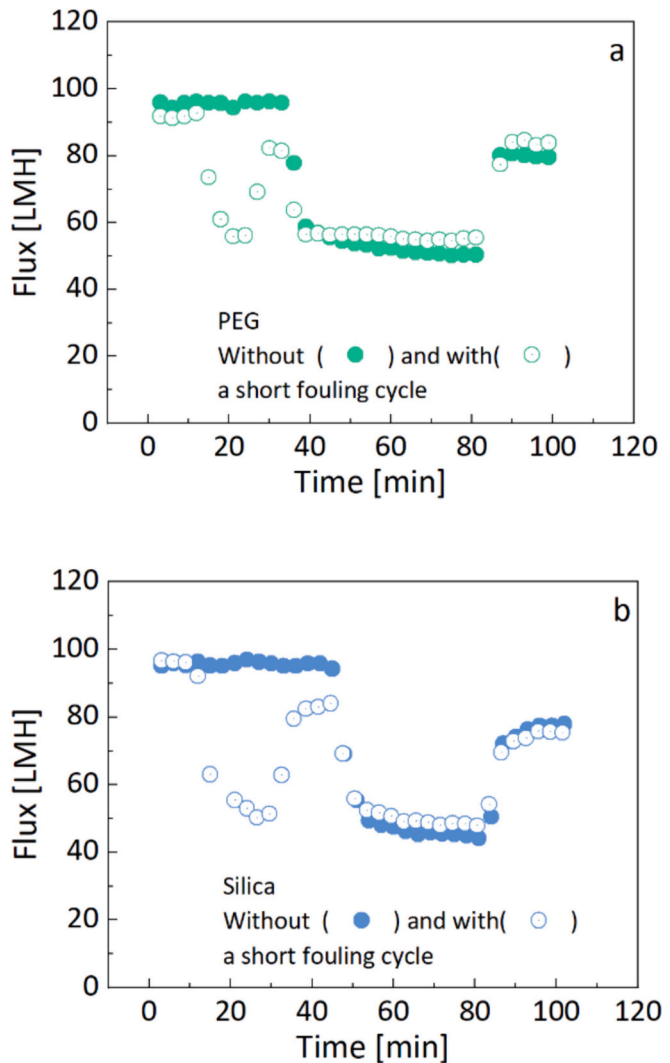


Fig. 5. Flux decline with (open symbols) and without (closed symbols) additional short-time fouling cycle for (a) 5 g/L PEG, and (b) 6 g/L silica.

values were given (Fig. S3a and b). As shown in Fig. S2, the calculated osmotic pressures of silica via Eq. (S3) were underestimated, because the contribution of counter ions to osmotic pressures was not considered in Carnahan-Stirling theory [68]. Consequently, the concentration of silica near the membrane wall will be overestimated when using Eq. (S3). As a result, it led to an overestimation of silica CP values, as shown in Fig. S3. This suggests that more attention should be paid to the relation between colloidal concentration and osmotic pressure, especially when colloids are with charges.

3.4. Effect of cross-flow velocity on CP mitigation

CP of both colloids were also evaluated via our method under various cross flow velocities (i.e., Re numbers), as shown in Fig. 8. CP values of both PEG and silica decreased as Re numbers increased from 3532 to 7317 (Fig. 8a). It is reported that CP can be mitigated at a high cross flow due to the promoted back diffusion process of solutes and the elevated shear forces [51,52,56]. However, compared to the Re , it was found that colloidal size played a more crucial role in CP. The CP value of silica, for example, was still as high as 250 under a high cross flow with Re number of 7317, which was higher than CP (48) of PEG at a small Re of 3532. Fig. 8b and c shows that as Re increased from 3532 to 7317, the contribution of CP to flux decline was reduced from 71 % to 50 % for PEG and from 48 % to 35 % for silica, suggesting that increasing the

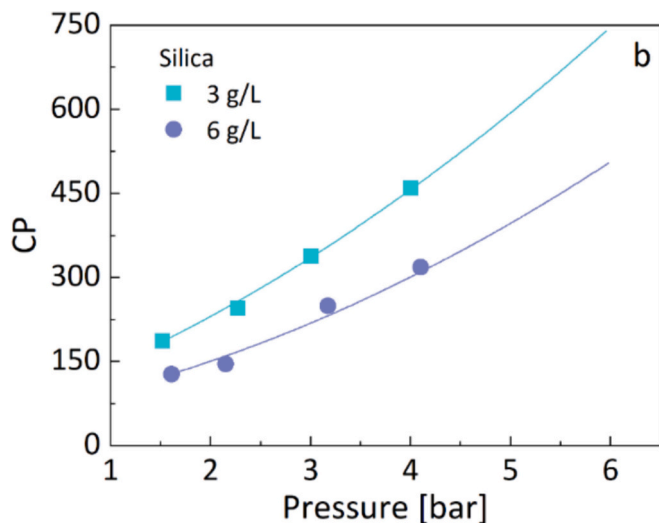
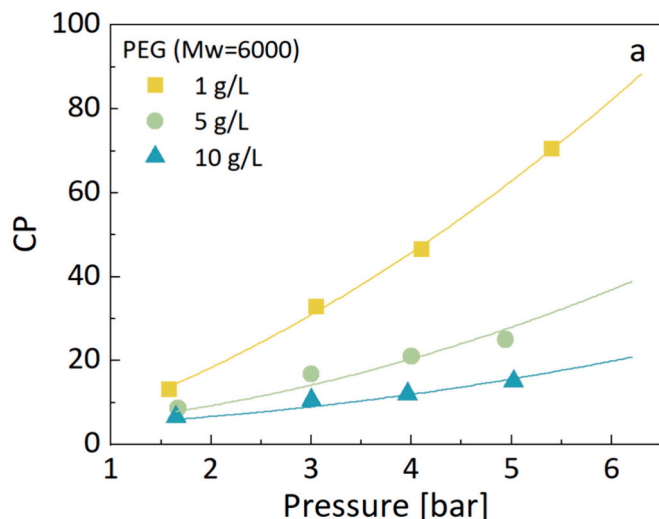


Fig. 6. CP was calculated from measurements at different transmembrane pressures for (a) PEG, and (b) silica with various concentrations at a constant cross flow velocity of 0.5 m/s.

cross-flow velocity can effectively mitigate the CP effect on flux. Although CP values (Fig. 8a) and CP contributions to flux decline (Fig. 8b and c), for the smaller-size colloids of PEG, were much smaller than that of silica, the normalized flux (Fig. S4) shows that the higher CP found in silica led to a more significant flux drop during the filtration of colloids. The prominent flux drop was probably attributed to the synergistic effect of CP and fouling because high CP caused by the larger-size colloids can facilitate fouling formation.

4. Conclusion

In this study, we proposed a new strategy to determine the contribution of fouling and CP to flux decline by comparing the pure water flux before and after filtering colloidal solutions with a ceramic NF membrane. CP values of PEG and silica colloids were evaluated via the osmotic pressures in the feed and near the membrane surface. The main conclusions were:

- Flux loss of 43–95 % during filtration of colloids was caused by CP-enhanced osmotic pressure near the membrane wall.

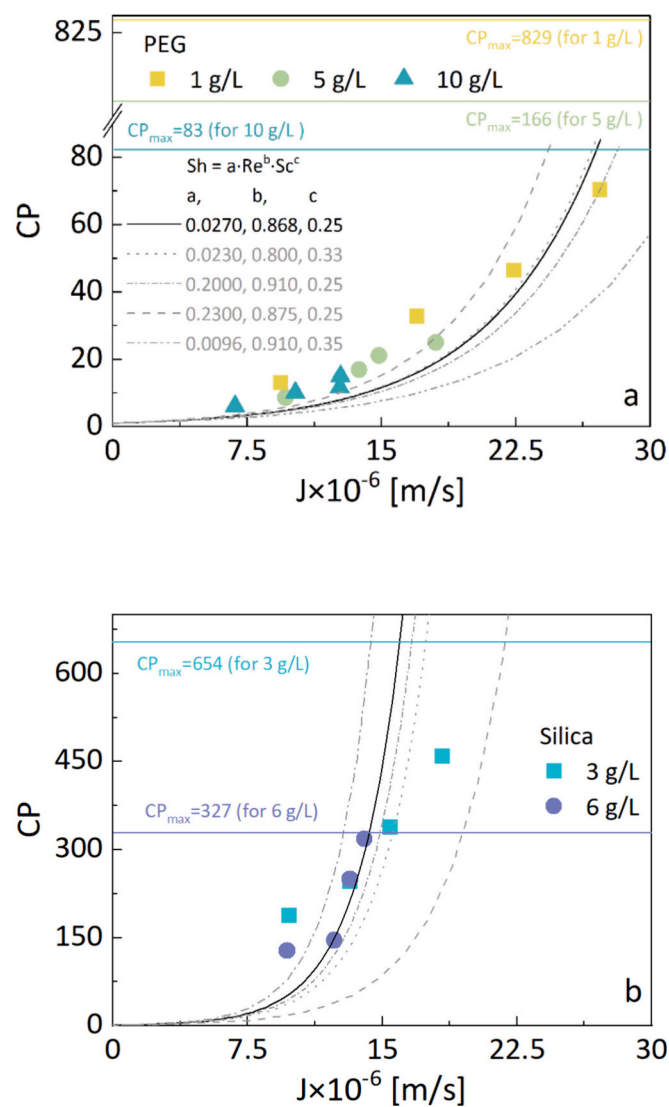


Fig. 7. Theoretical and experimental CP vs. flux for (a) 1, 5, and 10 g/L PEG, and (b) 3 and 6 g/L silica at a cross-flow velocity of 0.5 m/s. The solid curves in both (a) and (b) on behalf of the predicted CP profile were obtained through the film diffusion model by using the same calibrated Sherwood equation with calibrated constants of $a=0.027$, $b=0.868$, and $c=0.25$, while dashed lines represented the theoretical CP with flux via the film diffusion model through employing different Sherwood equations from literature [38,60–63].

- Silica colloids with a diameter of 10 nm, 3 times larger than PEG (2.9 nm), resulted in the largest CP due to the slow back diffusion from the membrane surface towards the bulk.
- CP values evaluated from the film diffusion model gave a deviation because the inaccurate K values calculated from the Sherwood equation were used in the model. In addition, CP values beyond the CP_{max} were calculated from the film diffusion model.
- CP of uncharged colloids like PEG was evaluated through the established relation between its high concentrations and osmotic pressures. However, CP prediction of hard spherical charged colloids like silica can be subject to the potential contribution of counter ions to osmotic pressure.
- As Re number increased at higher cross-flow velocities, the CP of the two colloids (PEG and silica) was decreased but remained at a high level, especially for the larger colloidal particles of silica.
- Contribution of CP to flux loss for silica can be reduced at a higher Re number. However, the effect of the higher CP resulting from larger-size colloids on fouling formation should be taken into account.

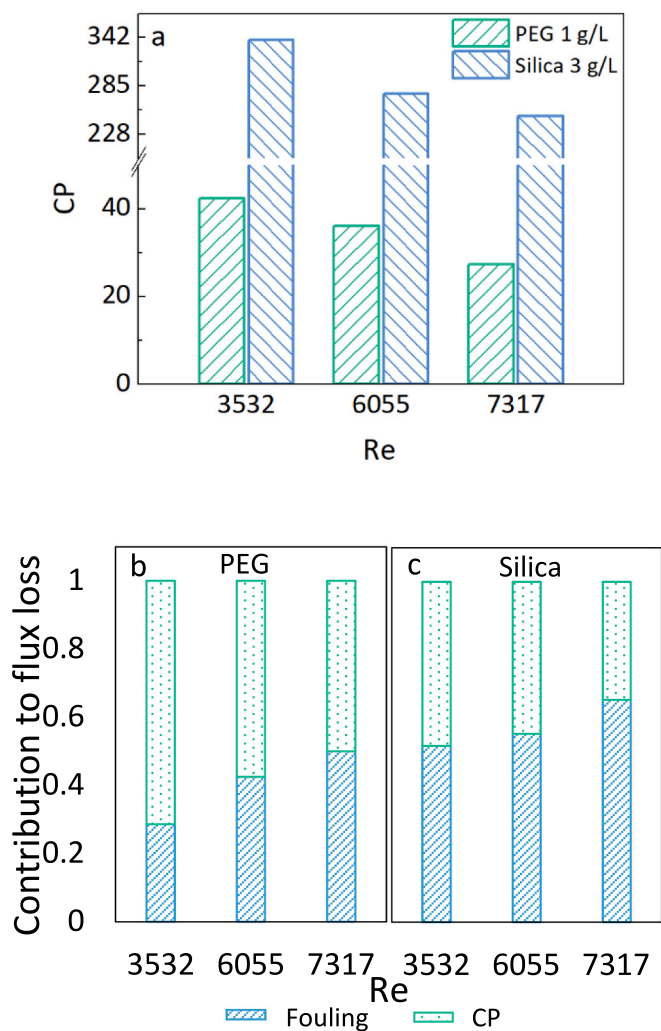


Fig. 8. (a) Experimental CP values with various Re numbers for 1 g/L PEG and 3 g/L silica, and contributions of CP and fouling to flux loss for (b) PEG and (c) silica.

CRediT authorship contribution statement

Shuo Zhang: Writing – review & editing, Writing – original draft, Methodology, Investigation, Formal analysis, Data curation, Conceptualization. **Xixin Liang:** Methodology, Investigation, Conceptualization. **Cai Yang:** Methodology. **Paul Venema:** Writing – review & editing, Methodology. **Luuk C. Rietveld:** Writing – review & editing, Supervision. **Sebastiaan G.J. Heijman:** Writing – review & editing, Supervision, Conceptualization.

Declaration of competing interest

The authors declare that they have no known competing financial interests or personal relationships that could have appeared to influence the work reported in this paper.

Data availability

Data will be made available on request.

Acknowledgement

The work was supported by China Scholarship Council (Grant number: 201808280006). Special thanks are given to Nadia van Pelt (TU

Delft, The Netherlands) for the help on language and grammar issues of the manuscript.

Appendix A. Supplementary data

Supplementary data to this article can be found online at <https://doi.org/10.1016/j.desal.2024.117722>.

References

- [1] B. Van Der Bruggen, C. Vandecasteele, T. Van Gestel, W. Doyen, R. Leysen, A review of pressure-driven membrane processes in wastewater treatment and drinking water production, *Environ. Prog.* 22 (2003) 46–56, <https://doi.org/10.1002/ep.670220116>.
- [2] A. Subramani, S. Kim, E.M.V. Hoek, Pressure, flow, and concentration profiles in open and spacer-filled membrane channels, *J. Membr. Sci.* 277 (2006) 7–17, <https://doi.org/10.1016/j.memsci.2005.10.021>.
- [3] S. Shirazi, C.J. Lin, D. Chen, Inorganic fouling of pressure-driven membrane processes — a critical review, *Desalination* 250 (2010) 236–248, <https://doi.org/10.1016/j.desal.2009.02.056>.
- [4] C.A. Hejase, V.V. Tarabara, Nanofiltration of saline oil-water emulsions: combined and individual effects of salt concentration polarization and fouling by oil, *J. Membr. Sci.* 617 (2021) 118607, <https://doi.org/10.1016/j.memsci.2020.118607>.
- [5] X. Li, D. Hasson, H. Shemer, Flow conditions affecting the induction period of CaSO₄ scaling on RO membranes, *Desalination* 431 (2018) 119–125, <https://doi.org/10.1016/j.desal.2017.08.014>.
- [6] E.M.V. Hoek, M. Elimelech, Cake-enhanced concentration polarization: a new fouling mechanism for salt-rejecting membranes, *Environ. Sci. Technol.* 37 (2003) 5581–5588, <https://doi.org/10.1021/es0262636>.
- [7] C.Y. Tang, T.H. Chong, A.G. Fane, Colloidal interactions and fouling of NF and RO membranes: a review, *Adv. Colloid Interf. Sci.* 164 (2011) 126–143, <https://doi.org/10.1016/j.cis.2010.10.007>.
- [8] L.M. Gowman, C. Ross Ethier, Concentration and concentration gradient measurements in an ultrafiltration concentration polarization layer part II: application to hyaluronan, *J. Membr. Sci.* 131 (1997) 107–123, [https://doi.org/10.1016/S0376-7388\(97\)00033-1](https://doi.org/10.1016/S0376-7388(97)00033-1).
- [9] A.N. Quay, T.Z. Tong, S.M. Hashmi, Y. Zhou, S. Zhao, M. Elimelech, Combined organic fouling and inorganic scaling in reverse osmosis: role of protein–silica interactions, *Environ. Sci. Technol.* 52 (2018) 9145–9153, <https://doi.org/10.1021/acs.est.8b02194>.
- [10] P. May, S. Laghmari, M. Ulbricht, Concentration polarization enabled reactive coating of nanofiltration membranes with zwitterionic hydrogel, *Membranes* 11 (2021) 187, <https://doi.org/10.3390/membranes11030187>.
- [11] C. Rey, N. Hengl, S. Baup, M. Karrouch, A. Dufresne, H. Djeridi, R. Dattani, F. Pignon, Velocity, stress and concentration fields revealed by micro-PIV and SAXS within concentration polarization layers during cross-flow ultrafiltration of colloidal laponite clay suspensions, *J. Membr. Sci.* 578 (2019) 69–84, <https://doi.org/10.1016/j.memsci.2019.02.019>.
- [12] M. Elimelech, S. Bhattacharjee, A novel approach for modeling concentration polarization in crossflow membrane filtration based on the equivalence of osmotic pressure model and filtration theory, *J. Membr. Sci.* 145 (1998) 223–241, [https://doi.org/10.1016/S0376-7388\(98\)00078-7](https://doi.org/10.1016/S0376-7388(98)00078-7).
- [13] S. Laghmari, P. May, M. Ulbricht, Polyzwitterionic hydrogel coating for reverse osmosis membranes by concentration polarization-enhanced in situ “click” reaction that is applicable in modules, *J. Membr. Sci.* 629 (2021) 119274, <https://doi.org/10.1016/j.memsci.2021.119274>.
- [14] V.S. Minnikanti, S. DasGupta, S. De, Prediction of mass transfer coefficient with suction for turbulent flow in cross flow ultrafiltration, *J. Membr. Sci.* 157 (1999) 227–239, [https://doi.org/10.1016/S0376-7388\(98\)00371-8](https://doi.org/10.1016/S0376-7388(98)00371-8).
- [15] S. Sablani, M. Goosens, R. Al-Belushi, M. Wilf, Concentration polarization in ultrafiltration and reverse osmosis: a critical review, *Desalination* 141 (2001) 269–289, [https://doi.org/10.1016/S0011-9164\(01\)85005-0](https://doi.org/10.1016/S0011-9164(01)85005-0).
- [16] Z. Zhou, B. Ling, I. Battiatto, S.M. Husson, D.A. Ladner, Concentration polarization over reverse osmosis membranes with engineered surface features, *J. Membr. Sci.* 617 (2021) 118199, <https://doi.org/10.1016/j.memsci.2020.118199>.
- [17] J. Liu, Z. Wang, C.Y. Tang, J.O. Leckie, Modeling dynamics of colloidal fouling of RO/NF membranes with a novel collision-attachment approach, *Environ. Sci. Technol.* 52 (2018) 1471–1478, <https://doi.org/10.1021/acs.est.7b05598>.
- [18] T.H. Chong, F.S. Wong, A.G. Fane, Implications of critical flux and cake enhanced osmotic pressure (CEOP) on colloidal fouling in reverse osmosis: experimental observations, *J. Membr. Sci.* 314 (2008) 101–111, <https://doi.org/10.1016/j.memsci.2008.01.030>.
- [19] P. Aimar, M. Meireles, P. Bacchin, V. Sanchez, Fouling and concentration polarization ultrafiltration and microfiltration, in: J.G. Crespo, K.W. Böddeker (Eds.), *Membr. Process. Sep. Purif.*, Springer Netherlands, Dordrecht, 1994, pp. 27–57, https://doi.org/10.1007/978-94-015-8340-4_3.
- [20] S. Kim, E.M.V. Hoek, Modeling concentration polarization in reverse osmosis processes, *Desalination* 186 (2005) 111–128, <https://doi.org/10.1016/j.desal.2005.05.017>.
- [21] L. Song, C. Liu, A total salt balance model for concentration polarization in crossflow reverse osmosis channels with shear flow, *J. Membr. Sci.* 401–402 (2012) 313–322, <https://doi.org/10.1016/j.memsci.2012.02.023>.

- [22] J.C. Chen, Q. Li, M. Elimelech, In situ monitoring techniques for concentration polarization and fouling phenomena in membrane filtration, *Adv. Colloid Interf. Sci.* 107 (2004) 83–108, <https://doi.org/10.1016/j.cis.2003.10.018>.
- [23] J.D. Nikolova, M.A. Islam, Contribution of adsorbed layer resistance to the flux-decline in an ultrafiltration process, *J. Membr. Sci.* 146 (1998) 105–111, [https://doi.org/10.1016/S0376-7388\(98\)00086-6](https://doi.org/10.1016/S0376-7388(98)00086-6).
- [24] P.M. Budd, 11 - polyelectrolytes, in: G. Allen, J.C. Bevington (Eds.), *Compr. Polym. Sci. Suppl.*, Pergamon, Amsterdam, 1989, pp. 215–230, <https://doi.org/10.1016/B978-0-08-096701-1.00011-2>.
- [25] T.H. Chong, F.S. Wong, A.G. Fane, Enhanced concentration polarization by unstirred fouling layers in reverse osmosis: detection by sodium chloride tracer response technique, *J. Membr. Sci.* 287 (2007) 198–210, <https://doi.org/10.1016/j.memsci.2006.10.035>.
- [26] T.O. Mahlangu, E.M.V. Hoek, B.B. Mamba, A.R.D. Verliefde, Influence of organic, colloidal and combined fouling on NF rejection of NaCl and carbamazepine: role of solute-foulant-membrane interactions and cake-enhanced concentration polarisation, *J. Membr. Sci.* 471 (2014) 35–46, <https://doi.org/10.1016/j.memsci.2014.07.065>.
- [27] K. Boussu, A. Belpaire, A. Volodin, C. Van Haesendonck, P. Van der Meeren, C. Vandecasteele, B. Van der Bruggen, Influence of membrane and colloid characteristics on fouling of nanofiltration membranes, *J. Membr. Sci.* 289 (2007) 220–230, <https://doi.org/10.1016/j.memsci.2006.12.001>.
- [28] Y.H. Cai, N. Galili, Y. Gelman, M. Herzberg, J. Gilron, Evaluating the impact of pretreatment processes on fouling of reverse osmosis membrane by secondary wastewater, *J. Membr. Sci.* 623 (2021) 119054, <https://doi.org/10.1016/j.memsci.2021.119054>.
- [29] W. Fan, F. Meneau, W. Bras, M. Ogura, G. Sankar, T. Okubo, Effects of silicon sources on the formation of nanosized LTA: an in situ small angle X-ray scattering and wide angle X-ray scattering study, *Microporous Mesoporous Mater.* 101 (2007) 134–141, <https://doi.org/10.1016/j.micromeso.2006.10.007>.
- [30] H. Liu, Y. Peng, C. Yang, M. Wang, Silica nanoparticles as adhesives for biological tissues? Re-examining the effect of particles size, particle shape, and the unexpected role of base, *Part. Part. Syst. Charact.* 34 (2017) 1700286, <https://doi.org/10.1002/ppsc.201700286>.
- [31] D. Airey, S. Yao, J. Wu, V. Chen, A.G. Fane, J.M. Pope, An investigation of concentration polarization phenomena in membrane filtration of colloidal silica suspensions by NMR micro-imaging, *J. Membr. Sci.* 145 (1998) 145–158, [https://doi.org/10.1016/S0376-7388\(98\)00051-9](https://doi.org/10.1016/S0376-7388(98)00051-9).
- [32] A. Jönsson, Concentration polarization and fouling during ultrafiltration of colloidal suspensions and hydrophobic solutes, *Sep. Sci. Technol.* 30 (1995) 301–312, <https://doi.org/10.1080/01496399508015840>.
- [33] J.Q.J.C. Verberk, Application of Air in Membrane Filtration (PhD thesis), Delft University of Technology, 2005, <http://resolver.tudelft.nl/uuid:034e4c75-dde-a-444b-837f-60fa179fee0a>. (Accessed 23 March 2022).
- [34] R.W. Field, J.J. Wu, Permeate flux in ultrafiltration processes—understandings and misunderstandings, *Membranes* 12 (2022) 187, <https://doi.org/10.3390/membranes12020187>.
- [35] Z. Alexandrowicz, Light-scattering measurement of the osmotic activity of a polyethylene glycol solution, *J. Polym. Sci.* 40 (1959) 107–112, <https://doi.org/10.1002/pol.1959.1204013607>.
- [36] L.W. Nichol, A.G. Ogston, B.N. Preston, The equilibrium sedimentation of hyaluronic acid and of two synthetic polymers, *Biochem. J.* 102 (1967) 407–416.
- [37] L.G. Peeva, E. Gibbins, S.S. Luthra, L.S. White, R.P. Stateva, A.G. Livingston, Effect of concentration polarisation and osmotic pressure on flux in organic solvent nanofiltration, *J. Membr. Sci.* 236 (2004) 121–136, <https://doi.org/10.1016/j.memsci.2004.03.004>.
- [38] I. Sutzkover, D. Hasson, R. Semiat, Simple technique for measuring the concentration polarization level in a reverse osmosis system, *Desalination* 131 (2000) 117–127, [https://doi.org/10.1016/S0011-9164\(00\)90012-2](https://doi.org/10.1016/S0011-9164(00)90012-2).
- [39] S. Bhatia, S. DasGupta, S. De, Performance prediction of membrane modules incorporating the effects of suction in the mass transfer coefficient under turbulent flow conditions, *Sep. Purif. Technol.* 55 (2007) 182–190, <https://doi.org/10.1016/j.seppur.2006.11.020>.
- [40] V. Gekas, K. Ölund, Mass transfer in the membrane concentration polarization layer under turbulent cross flow: II. Application to the characterization of ultrafiltration membranes, *J. Membr. Sci.* 37 (1988) 145–163, [https://doi.org/10.1016/S0376-7388\(00\)83069-0](https://doi.org/10.1016/S0376-7388(00)83069-0).
- [41] M.S.H. Bader, J.N. Veenstra, Analysis of concentration polarization phenomenon in ultrafiltration under turbulent flow conditions, *J. Membr. Sci.* 114 (1996) 139–148, [https://doi.org/10.1016/0376-7388\(95\)00136-0](https://doi.org/10.1016/0376-7388(95)00136-0).
- [42] E. Dražević, K. Koštić, V. Dananić, Mass transfer of differently sized organic solutes at spacer covered and permeable nanofiltration wall, *Chem. Eng. J.* 244 (2014) 152–159, <https://doi.org/10.1016/j.cej.2014.01.043>.
- [43] B. Lin, S.G.J. Heijman, R. Shang, L.C. Rietveld, Integration of oxalic acid chelation and Fenton process for synergistic relaxation-oxidation of persistent gel-like fouling of ceramic nanofiltration membranes, *J. Membr. Sci.* 636 (2021) 119553, <https://doi.org/10.1016/j.memsci.2021.119553>.
- [44] I. Koyuncu, D. Topacik, M.R. Wiesner, Factors influencing flux decline during nanofiltration of solutions containing dyes and salts, *Water Res.* 38 (2004) 432–440, <https://doi.org/10.1016/j.watres.2003.10.001>.
- [45] P. Bacchin, M. Meireles, P. Aimar, Modelling of filtration: from the polarised layer to deposit formation and compaction, *Desalination* 145 (2002) 139–146, [https://doi.org/10.1016/S0011-9164\(02\)00399-5](https://doi.org/10.1016/S0011-9164(02)00399-5).
- [46] L.D. Nghiem, A.I. Schäfer, Adsorption and transport of trace contaminant estrone in NF/RO membranes, *Environ. Eng. Sci.* 19 (2002) 441–451, <https://doi.org/10.1089/109287502320963427>.
- [47] V. Chen, A.G. Fane, S. Madaeni, I.G. Wenten, Particle deposition during membrane filtration of colloids: transition between concentration polarization and cake formation, *J. Membr. Sci.* 125 (1997) 109–122, [https://doi.org/10.1016/S0376-7388\(96\)00187-1](https://doi.org/10.1016/S0376-7388(96)00187-1).
- [48] K. Akamatsu, Y. Kagami, S. Nakao, Effect of BSA and sodium alginate adsorption on decline of filtrate flux through polyethylene microfiltration membranes, *J. Membr. Sci.* 594 (2020) 117469, <https://doi.org/10.1016/j.memsci.2019.117469>.
- [49] E. Matthiasson, The role of macromolecular adsorption in fouling of ultrafiltration membranes, *J. Membr. Sci.* 16 (1983) 23–36, [https://doi.org/10.1016/S0376-7388\(00\)81297-1](https://doi.org/10.1016/S0376-7388(00)81297-1).
- [50] L. Wang, L. Song, Flux decline in crossflow microfiltration and ultrafiltration: experimental verification of fouling dynamics, *J. Membr. Sci.* 160 (1999) 41–50, [https://doi.org/10.1016/S0376-7388\(99\)00075-7](https://doi.org/10.1016/S0376-7388(99)00075-7).
- [51] G. Yang, W. Xing, N. Xu, Concentration polarization in spiral-wound nanofiltration membrane elements, *Desalination* 154 (2003) 89–99, [https://doi.org/10.1016/S0011-9164\(03\)00210-8](https://doi.org/10.1016/S0011-9164(03)00210-8).
- [52] T.Y. Qiu, P.A. Davies, Concentration polarization model of spiral-wound membrane modules with application to batch-mode RO desalination of brackish water, *Desalination* 368 (2015) 36–47, <https://doi.org/10.1016/j.desal.2014.12.048>.
- [53] J. Luo, L. Ding, Y. Su, S. Wei, Y. Wan, Concentration polarization in concentrated saline solution during desalination of iron dextran by nanofiltration, *J. Membr. Sci.* 363 (2010) 170–179, <https://doi.org/10.1016/j.memsci.2010.07.033>.
- [54] J. Fernández-Sempere, F. Ruiz-Beviá, P. García-Algado, R. Salcedo-Díaz, Visualization and modelling of the polarization layer and a reversible adsorption process in PEG-10000 dead-end ultrafiltration, *J. Membr. Sci.* 342 (2009) 279–290, <https://doi.org/10.1016/j.memsci.2009.06.046>.
- [55] R. Salcedo-Díaz, P. García-Algado, M. García-Rodríguez, J. Fernández-Sempere, F. Ruiz-Beviá, Visualization and modeling of the polarization layer in crossflow reverse osmosis in a slit-type channel, *J. Membr. Sci.* 456 (2014) 21–30, <https://doi.org/10.1016/j.memsci.2014.01.019>.
- [56] E.M.V. Hoek, A.S. Kim, M. Elimelech, Influence of crossflow membrane filter geometry and shear rate on colloidal fouling in reverse osmosis and nanofiltration separations, *Environ. Eng. Sci.* 19 (2002) 357–372, <https://doi.org/10.1089/109287502320963364>.
- [57] W.R. Bowen, F. Jenner, Theoretical descriptions of membrane filtration of colloids and fine particles: an assessment and review, *Adv. Colloid Interf. Sci.* 56 (1995) 141–200, [https://doi.org/10.1016/0001-8686\(94\)00232-2](https://doi.org/10.1016/0001-8686(94)00232-2).
- [58] J. Liu, T. Huang, R. Ji, Z. Wang, C.Y. Tang, J.O. Leckie, Stochastic collision–attachment-based Monte Carlo simulation of colloidal fouling: transition from foulant–clean–membrane interaction to foulant–fouled–membrane interaction, *Environ. Sci. Technol.* 54 (2020) 12703–12712, <https://doi.org/10.1021/acs.est.0c04165>.
- [59] E.S. Jang, W. Mickols, R. Sujanani, A. Helenic, T.J. Dilenschneider, J. Kamcev, D. R. Paul, B.D. Freeman, Influence of concentration polarization and thermodynamic non-ideality on salt transport in reverse osmosis membranes, *J. Membr. Sci.* 572 (2019) 668–675, <https://doi.org/10.1016/j.memsci.2018.11.006>.
- [60] V. Gekas, B. Hallström, Mass transfer in the membrane concentration polarization layer under turbulent cross flow: I. Critical literature review and adaptation of existing sherwood correlations to membrane operations, *J. Membr. Sci.* 30 (1987) 153–170, [https://doi.org/10.1016/S0376-7388\(00\)81349-6](https://doi.org/10.1016/S0376-7388(00)81349-6).
- [61] E.E. Chang, C.H. Liang, C.P. Huang, P.C. Chiang, A simplified method for elucidating the effect of size exclusion on nanofiltration membranes, *Sep. Purif. Technol.* 85 (2012) 1–7, <https://doi.org/10.1016/j.seppur.2011.05.002>.
- [62] G.B. van den Berg, I.G. Rácz, C.A. Smolders, Mass transfer coefficients in cross-flow ultrafiltration, *J. Membr. Sci.* 47 (1989) 25–51, [https://doi.org/10.1016/S0376-7388\(00\)80585-3](https://doi.org/10.1016/S0376-7388(00)80585-3).
- [63] A. Imbrogno, A.I. Schäfer, Comparative study of nanofiltration membrane characterization devices of different dimension and configuration (cross flow and dead end), *J. Membr. Sci.* 585 (2019) 67–80, <https://doi.org/10.1016/j.memsci.2019.04.035>.
- [64] P. Persoff, J. Apps, G. Moridis, J.M. Whang, Effect of dilution and contaminants on sand grouted with colloidal silica, *J. Geotech. Geoenviron. Eng.* 125 (1999) 461–469, [https://doi.org/10.1061/\(ASCE\)1090-0241\(1999\)125:6\(461\)](https://doi.org/10.1061/(ASCE)1090-0241(1999)125:6(461)).
- [65] P. Bacchin, P. Aimar, R.W. Field, Critical and sustainable fluxes: theory, experiments and applications, *J. Membr. Sci.* 281 (2006) 42–69, <https://doi.org/10.1016/j.memsci.2006.04.014>.
- [66] J. Luo, L. Ding, Y. Wan, P. Paullier, M.Y. Jaffrin, Fouling behavior of dairy wastewater treatment by nanofiltration under shear-enhanced extreme hydraulic conditions, *Sep. Purif. Technol.* 88 (2012) 79–86, <https://doi.org/10.1016/j.seppur.2011.12.008>.
- [67] C. Pasquier, S. Beaujalis, A. Bouchoux, S. Rigault, B. Cabane, M. Lund, V. Lechevalier, C.L. Floch-Foutré, M. Pasco, G. Pabœuf, J. Pérez, S. Pezennec, Osmotic pressures of lysozyme solutions from gas-like to crystal states, *Phys. Chem. Chem. Phys.* 18 (2016) 28458–28465, <https://doi.org/10.1039/C6CP03867K>.
- [68] B. Jönsson, J. Persello, J. Li, B. Cabane, Equation of state of colloidal dispersions, *Langmuir* 27 (2011) 6606–6614, <https://doi.org/10.1021/la2001392>.